The Journal of Immunology

Small Ubiquitin-like Modifier Alters IFN Response

Ghizlane Maarifi, Mohamed Ali Maroui, Jacques Dutrieux, Laurent Dianoux, Sébastien Nisole and Mounira K. Chelbi-Alix

J Immunol 2015; 195:2312-2324; Prepublished online 29 July 2015;
doi: 10.4049/jimmunol.1500035
http://www.jimmunol.org/content/195/5/2312

The Journal of Immunology is published twice each month by
The American Association of Immunologists, Inc.,
1451 Rockville Pike, Suite 650, Rockville, MD 20852

Print ISSN: 0022-1767 Online ISSN: 1550-6606.

Small Ubiquitin-like Modifier Alters IFN Response

Ghizlane Maarifi, Mohamed Ali Maroui, Jacques Dutrieux, Laurent Dianoux, Sébastien Nisole, and Mounira K. Chelbi-Alix

IFNs orchestrate immune defense through induction of hundreds of genes. Small ubiquitin-like modifier (SUMO) is involved in various cellular functions, but little is known about its role in IFN responses. Prior work identified STAT1 SUMOylation as an important mode of regulation of IFN-γ signaling. In this study, we investigated the roles of SUMO in IFN signaling, gene expression, protein stability, and IFN-induced biological responses. We first show that SUMO overexpression leads to STAT1 SUMOylation and to a decrease in IFN-induced STAT1 phosphorylation. Interestingly, IFNs exert a negative retrocontrol on their own signaling by enhancing STAT1 SUMOylation. Furthermore, we show that expression of each SUMO paralog inhibits IFN-γ–induced transcription without affecting that of IFN-α. Further, we focused on IFN-induced gene products associated to promyelocytic leukemia (PML) nuclear bodies, and we show that neither IFN-α nor IFN-γ could increase PML and Sp100 protein expression because they enhanced their SUMO3 conjugation and subsequent proteasomal degradation. Because it is known that SUMO3 is important for the recruitment of RING finger protein 4, a poly–SUMO-dependent E3 ubiquitin ligase, and that PML acts as a positive regulator of IFN-induced STAT1 phosphorylation, we went on to show that RING finger protein 4 depletion stabilizes PML and is correlated with a positive regulation of IFN signaling. Importantly, inhibition of IFN signaling by SUMO is associated with a reduction of IFN-induced apoptosis, cell growth inhibition, antiviral defense, and chemotaxis. Conversely, inhibition of SUMOylation results in higher IFN-γ–induced STAT1 phosphorylation and biological responses. Altogether, our results uncover a new role for SUMO in the modulation of IFN response. *The Journal of Immunology*, **2015, 195: 2312–2324.**

Interferons are a family of cytokines that exhibit diverse biological activities. Identified and named for their antiviral properties, IFNs have also immunomodulatory, antiproliferative, and apoptotic activities (1). IFNs are successfully used in therapy to treat viral infections, cancer, or multiple sclerosis. However, the use of IFN is limited and some patients are resistant to treatment. Thus, progress remains to be done to better understand the mechanism of action of IFNs.

Based on their structure and interaction with distinct receptor complexes, IFNs are subdivided into three distinct types. IFNs consist in multiple type I species (including IFN-α and IFN-β), one type II (IFN-γ), and three members of type III species (IFN-λs, also known as IL-28 and -29) (2). IFNs act on cells by binding to their respective receptors (IFN-α receptor [IFNAR] for IFN-α/β, IFNGR for IFN-γ, or IFNLR for IFN-λ) and activating the JAK/STAT pathways to trigger the transcription of >300 IFN-stimulated genes (ISGs), the products of which are the mediators of their biological effects (2). The interaction of IFN-α/β with IFNAR leads to the activation of the JAK tyrosine kinases (Tyk2 and JAK1) that phosphorylate STAT1 and STAT2. Phosphorylated STATs heterodimerize and form with the DNA binding protein IFN regulatory factor 9 (IRF9), a complex called IFN-stimulated growth factor 3 (ISGF3). ISGF3 translocates into the nucleus to induce ISGs harboring an IFN-stimulated response element (ISRE). The binding of IFN-γ to its receptor, IFNGR, results in the phosphorylation of STAT1 by JAK1 and JAK2. p-STAT1 on Tyr^{701} forms homodimers that migrate to the nucleus and bind to a DNA element termed γ-activated sequence (GAS) in the promoter of specific ISGs. Accordingly, transcriptional responses to IFN-γ are dominated by the activity of pSTAT1 homodimers. Finally, type III IFNs that are structurally and genetically distinct from type I IFNs bind to different receptors, but activate the same signal transduction pathway (2).

The signal transduction induced by IFNs is transient because it is inhibited by negative regulators of IFN signaling that include phosphotyrosine phosphatases (Src homology region 2 domain-containing phosphatases, CD45, and PTP1B/TC-PTP), suppressors of cytokine signaling, and protein inhibitors of activated STATs (PIAS), which ensure the proper termination of IFN response (3).

Ubiquitin or ubiquitin-like proteins, such as SUMO or ISG15, modify many ISGs or key regulators of IFN signaling (4). However, the role of SUMO on IFN-induced signaling, cell growth inhibition, apoptosis, and antiviral activity remains to be elucidated. SUMOylation is the posttranslational covalent but reversible conjugation of SUMO to proteins. In humans, the SUMO protein family consists of SUMO1 and two highly homologous proteins SUMO2 and SUMO3 (collectively called SUMO2/3), which cannot be distinguished by currently available Abs. SUMO2 and SUMO3 share 97% sequence identity and are expressed at much higher levels than SUMO1, with which they only share ∼50% identity (5).

INSERM Unité Mixte de Recherche S 1124, Université Paris Descartes, 75006 Paris, France

Received for publication January 12, 2015. Accepted for publication June 17, 2015.

This work was supported by the Agence Nationale de la Recherche (ANR 11BSV3002803). M.A.M. is supported by the Agence Nationale de la Recherche. J.D. is supported by the Agence Nationale de la Recherche sur le SIDA et les Hépatites Virales.

Address correspondence and reprint requests to Dr. Sébastien Nisole and Dr. Mounira K. Chelbi-Alix, INSERM Unité Mixte de Recherche S 1124, Université Paris Descartes, 45 rue des Saints-Pères, 75006 Paris, France. E-mail addresses: sebastien.nisole@inserm.fr (S.N.) and mounira.chelbi-alix@parisdescartes.fr (M.K.C.-A.)

The online version of this article contains supplemental material.

Abbreviations used in this article: EMCV, encephalomyocarditis virus; F, forward; GAS, γ-activated sequence; IFNAR, IFN-α receptor; IP-10, IFN-γ–induced protein 10; IRF, IFN regulatory factor; ISG, IFN-stimulated gene; ISGF3, IFN-stimulated growth factor 3; ISRE, IFN-stimulated response element; MOI, multiplicity of infection; NB, nuclear body; PI, propidium iodide; PIAS, protein inhibitor of activated STATs; PKR, RNA-dependent protein kinase; PML, promyelocytic leukemia; qRT-PCR, quantitative RT-PCR; R, reverse; RNF4, RING finger protein 4; siRNA, small interfering RNA; SUMO, small ubiquitin-like modifier; TAP1, transporter associated with Ag processing 1; $TCID_{50}$, 50% tissue culture infective dose; wt, wild-type.

SUMO modification occurs through the formation of an isopeptide bond between the α-amino group of a lysine residue from the substrate and the C terminus COOH group of SUMO. SUMOylation involves a complex network of SUMO-activating enzymes (1 and 2), conjugating enzyme (Ubc9), and SUMO-E3 ligases (PIAS1, PIAS3, PIASxα, PIASxβ, PIASy, RanBP2, and Pc2) (6). The dynamic protein SUMOylation is counterbalanced by SUMO-specific proteases, which cleave SUMO moieties on specific substrates. SUMOylation leads to significant structural and conformational changes of the substrate by masking or conferring additional scaffolding surfaces for protein interactions. This posttranslational modification is involved in the regulation of intracellular trafficking, cell cycle, DNA repair, cell signaling, and protein degradation (5).

At present, little is known about the role of SUMO on IFN responses. STAT1 was found to be conjugated to SUMO on Lys^{703} by PIAS (7–9). Several studies reported that the activity of STAT1 could be inhibited by SUMO conjugation, because a SUMOylation-deficient STAT1 mutant is hyperphosphorylated and has higher DNA binding on STAT1-responsive gene promoters (8, 10, 11). However, whether increased cellular protein conjugation to SUMO could alter IFN signaling, stability of ISG products or IFN responses remains unknown. To better understand the role of SUMOylation in type I and II IFN pathways, we stably overexpressed each SUMO paralog in human cells and investigated the consequences on IFN signaling and IFN transcriptional responses. We also tested the capacity of IFN to regulate its own signaling and analyzed the fate of some ISG products, including promyelocytic leukemia (PML) nuclear body (NB)–associated proteins. Finally, we assessed the effects of SUMO on IFN-induced biological activities such as cell growth and viral inhibition, apoptosis, and IFN-γ–induced protein 10 (IP-10)–induced chemotaxis.

Materials and Methods

Materials

Recombinant human IFN-α2 was from Schering, human IFN-γ from Roussel Uclaf (Romainville, France), and ginkgolic acid from Merck. Mouse monoclonal anti-PML (sc-966) and anti–IP-10 (sc-101500) Abs and rabbit polyclonal Abs raised against PML (Sc-5621), STAT1 (C-STAT1 Ab) (sc-345), STAT1 phosphotyrosine 701 (sc-7988), RNA-dependent protein kinase (PKR; sc-707), IRF1 (sc-497), SUMO1 (sc-9060), and transporter associated with Ag processing 1 (TAP1; sc-20930) were from Santa Cruz Biotechnology. Rabbit anti-STAT2 and anti-STAT2 phosphotyrosine 689 Abs were obtained from Upstate Biotechnology. Monoclonal anti-STAT1 Ab (MA1-19371) (N-STAT1Ab) recognizing an epitope included within aa 8–23 of STAT1 was from Life Technologies. Mouse anti-6His Abs were from Clontech and rabbit anti-SUMO2/3 Abs used for Western blot from Invitrogen. Peroxidase-coupled secondary Abs were purchased from Santa Cruz Biotechnology. Mouse anti-6His Abs used for immunofluorescence were from Thermo Scientific. Rabbit anti-SUMO2/3 Abs used for immunofluorescence were a gift from Mary Dasso and Maia Ouspenskaia (National Institutes of Health, Bethesda, MD). Rabbit anti-Sp100 Abs were a gift from Hans Will (Leibniz Institute for Experimental Virology, Hamburg, Germany), and rabbit anti-EMCV Abs were from Ann Palmenberg (University of Wisconsin–Madison, Madison, WI). Secondary Abs conjugated to Alexa Fluor were purchased from Molecular Probes. Encephalomyocarditis virus (EMCV) was produced as previously described (12). Plasmid transfections were performed using Fugene 6 (Promega). Small interfering RNA (siRNA) targeting PML, Ubc9, or RING finger protein 4 (RNF4) were purchased from GE Healthcare (ON-TARGETplus siRNA SMARTpool) and transfected into cells using HiperFect transfection reagent (Qiagen). IP-10 was quantified in cell culture medium using CXCL10/IP-10 Immunoassay (Quantikine ELISA; R&D Systems). Luciferase assays were performed using the Luciferase Assay System (Promega) following the manufacturer's instructions. Cell proliferation was evaluated using the Cell Proliferation Kit I (MTT) purchased from Roche. Confocal laser microscopy was performed on a Zeiss LSM 710 microscope (Carl Zeiss).

Cells

Human glioblastoma astrocytoma U373MG, cervical cancer HeLa, and hepatocellular carcinoma HepG2 cells were grown at 37°C in DMEM supplemented with 10% FCS. His-SUMO constructs were generated by inserting each cDNA encoding SUMO paralog in pcDNA3.1. In accordance with the National Center for Biotechnology Information database, we refer to the entry P63165 as SUMO1, P61956 as SUMO2, and P55854 as SUMO3. HeLa and U373MG cells stably expressing each SUMO paralog were obtained by transfection with pcDNA SUMO constructs and subsequent neomycine selection (0.5 mg/ml).

Purification of His_6-tagged SUMO conjugates

Cells (10^7) untreated or treated with 1000 U/ml IFN for 30 min were lysed in denaturating buffer A (6 mol guanidinium-HCl, 0.1 mol Na_2HPO_4/NaH_2PO_4, 0.01 mol Tris-HCl [pH 8], 5 mmol imidazole, and 10 mmol 2-ME). After sonication, the lysates were mixed with 50 μl Ni-NTA-agarose beads (Qiagen) for 3 h at room temperature. The beads were successively washed with buffer B (0.1% Triton X-100, 8 mol urea, 0.1 mol Na_2HPO_4/NaH_2PO_4, 0.01 mol Tris-HCl [pH 6.3], and 10 mmol 2-ME), and subsequently eluted with 200 mmol imidazole in 0.15 mol Tris-HCl (pH 6.7), 30% glycerol, and 0.72 mol 2-ME.

EMSA

Control cells and cells stably expressing SUMO1 or SUMO3 were left untreated or treated with 1000 U/ml IFN-γ or IFN-α for 30 min. Cells (3×10^7) were harvested, and nuclear cell extracts were prepared using the NucBuster Protein Extraction Kit from Novagen. Proteins were examined by EMSA with a ^{32}P-labeled GAS probe or ^{32}P-labeled ISRE probe. The GAS probe was generated with the following duplex oligonucleotide: 5′-TACAACAGCCTGAT*TTCCCCGAA*ATGACGC-3′ (the GAS-like site is italicized). The ISRE probe was generated with the duplex oligonucleotide 5′-AAAGGGAAAGTGAAACTAGAAAGTGAAAGA-3′. The presence of specific GAF or ISGF3 complexes was confirmed with specific anti-STAT1 or anti-STAT2 Abs. The reaction products were analyzed by electrophoresis in a 4% nondenaturing polyacrylamide gel. The gel was dried and analyzed by PhosphorImager.

Virus stocks and cell infection

EMCV (4×10^8 PFU/ml) titer was determined by standard plaque assays. HeLa-wt, HeLa-SUMO1, or HeLa-SUMO3 cells were grown on glass coverslips in six-well plates (from 50–80% confluence) and infected with EMCV at the multiplicities of infection (MOIs) and at times postinfection indicated in the figure legends. Viral titers were determined on HeLa cells by measuring the 50% tissue culture infective dose ($TCID_{50}$).

Real-time PCR

Total RNAs were extracted using RNeasy Mini Kit (Qiagen) following the manufacturer's instructions. RNA samples were converted to cDNA using the RevertAid H Minus First Strand cDNA Synthesis Kit (Thermo Scientific). Real-time PCR reactions were performed in duplicates using 5 μl cDNA diluted 10 times in water using Takyon ROX SYBR MasterMix blue dTTP (Eurogentec). The following program was used on a 7900HT Fast Real-Time PCR System (Applied Biosystems): 3 min at 95°C followed by 35 cycles of 15 s at 95°C, 25 s at 60°C, and 25 s at 72°C. Values for each transcript were normalized to expression levels of RPL13A (60S ribosomal protein L13a) using the 2-ΔΔCt method. Primers used for quantification of transcripts by real-time quantitative PCR are as follows: STAT1 forward (F), 5′-CAGAGCCAATGGAACTTGATGG-3′ and STAT1 reverse (R), 5′-TCCGAGACACCTCGTCAAACTC-3′; IRF1-F, 5′-ACTTTC-GCTGTGCCATGAACTC-3′ and IRF1-R, 5′-CGGCTGGACTTCGACTTT-CTTT-3′; PML-F, 5′- ACACCAGTGGTTCCTCAAGCA-3′ and PML-R, 5′-CTCGGCAGTAGATGCTGGTCA-3′; PKR-F, 5′-GCGATACATGAGCC-CAGAACAG-3′ and PKR-R, 5′-CTGAGATGATGCCATCCCGTAG-3′; TAP1-F, 5′-TCCTGGTGGTCCTCTCCTCTCT-3′ and TAP1-R, 5′-CACTGCACTGGC-TATGGTGAGA-3′; and IP-10–F, 5′-CGCTGTACCTGCATCAGCAT-3′ and IP-10–R, 5′-GCAATGATCTCAACACGTGGAC-3′.

Immunofluorescence analysis

Cells grown on glass coverslip were fixed 20 min with 4% paraformaldehyde in PBS and permeabilized for 5 min in 0.1% Triton X-100 in PBS. Cells were then prepared for immunofluorescence staining using the appropriate primary Ab and the corresponding secondary Ab conjugated to Alexa Fluor (Molecular Probes). Cells were mounted onto glass slides by using Immu-Mount (Shandon) containing DAPI. Confocal laser microscopy was performed on a Zeiss LSM 710 microscope (Carl Zeiss).

Apoptosis

Cell apoptosis was assessed using the Annexin V-FITC/PI Kit (BD Biosciences). Briefly, HepG2 cells were transfected with 0.5 ng SUMO3-YFP or pcDNA3 constructs. After 24 h, cells were left untreated or treated with 1000 U/ml IFN-α or IFN-γ for 72 h, and HeLa-wt, HeLa-SUMO1, and HeLa-SUMO3 were untreated or treated with 1000 U/ml IFN-γ for 72 h. Cells were collected, resuspended in 100 μl PBS, and stained with Annexin V for 15 min at 4˚C, followed by propidium iodide (PI) staining. Ten thousand cells were analyzed by flow cytometry on an FACSCalibur (BD Biosciences).

In vitro chemotaxis assay

HeLa cells or cells stably expressing SUMO1 or SUMO3 were seeded at 10^5 cells/well CELLSTAR 12-well cell culture plates. Cells were left untreated or treated with 1000 U/ml IFN-γ. Seventy-two hours later, 12-well ThinCert cell culture inserts (Greiner Bio-One) were inserted into the wells. CD3/CD28-activated human CD4 T lymphocytes (5×10^5) were added to each well culture insert and incubated for 6 h. Cells that migrated into the lower chambers were collected and counted on a flow cytometer. Cell migration rates were determined by calculating the percentage of input cells that migrated into the lower chamber.

Results

IFN-induced STAT1 phosphorylation is reduced by SUMO

In order to investigate the impact of SUMO on the cellular response to IFN, we generated HeLa cells stably expressing His-SUMO1 (HeLa-SUMO1) or His-SUMO3 (HeLa-SUMO3) and U373MG cells stably expressing His-SUMO2 (U373MG-SUMO2) or His-SUMO3 (U373MG-SUMO3). Immunofluorescence and Western blot analyses confirmed an enrichment of the expression of each SUMO paralog compared with wild-type (wt) cells (Supplemental Fig. 1 and data not shown). Western blot analysis showed a marked increase of free SUMO expression as well as the proportion of SUMO-conjugated proteins in HeLa (Supplemental Fig. 1A) and U373MG (Supplemental Fig. 1B) cells. Immunofluorescence analysis revealed that SUMO1, SUMO2, or SUMO3 were found in nuclear speckles named PML NBs, as expected (Supplemental Fig. 1C, 1D).

Next, we sought to determine the effect of SUMO expression on IFN signaling by analyzing STAT1 tyrosine phosphorylation. HeLa and U373MG wt cells and cells overexpressing SUMO1, SUMO2, or SUMO3 were treated with IFN-α or IFN-γ for 30 min and the corresponding protein extracts analyzed by Western blot. As anticipated, IFN-γ (Fig. 1A, 1B) and IFN-α (Fig. 1C, 1D) induced a robust increase in p-STAT1 in wt cells. The induction of pSTAT1 in response to IFN-γ was markedly reduced in cells expressing SUMO1 (Fig. 1A), SUMO2 (Supplemental Fig. 1E), or SUMO3 (Fig. 1B). A similar reduction in STAT1 phosphorylation was observed in cells overexpressing SUMO1 (Fig. 1C), SUMO2 (Supplemental Fig. 1E), or SUMO3 (Fig. 1D) in response to IFN-α. In contrast, the IFN-α–induced phosphorylation of STAT2 was insensitive to SUMO (Fig. 1C, 1D, Supplemental Fig. 1E).

In a converse experiment, we examined the impact of the inhibition of SUMOylation on IFN-induced STAT1 phosphorylation. For this purpose, HeLa-wt cells were either treated with ginkgolic acid (Fig. 1E, 1F) that directly binds E1 and inhibits the formation

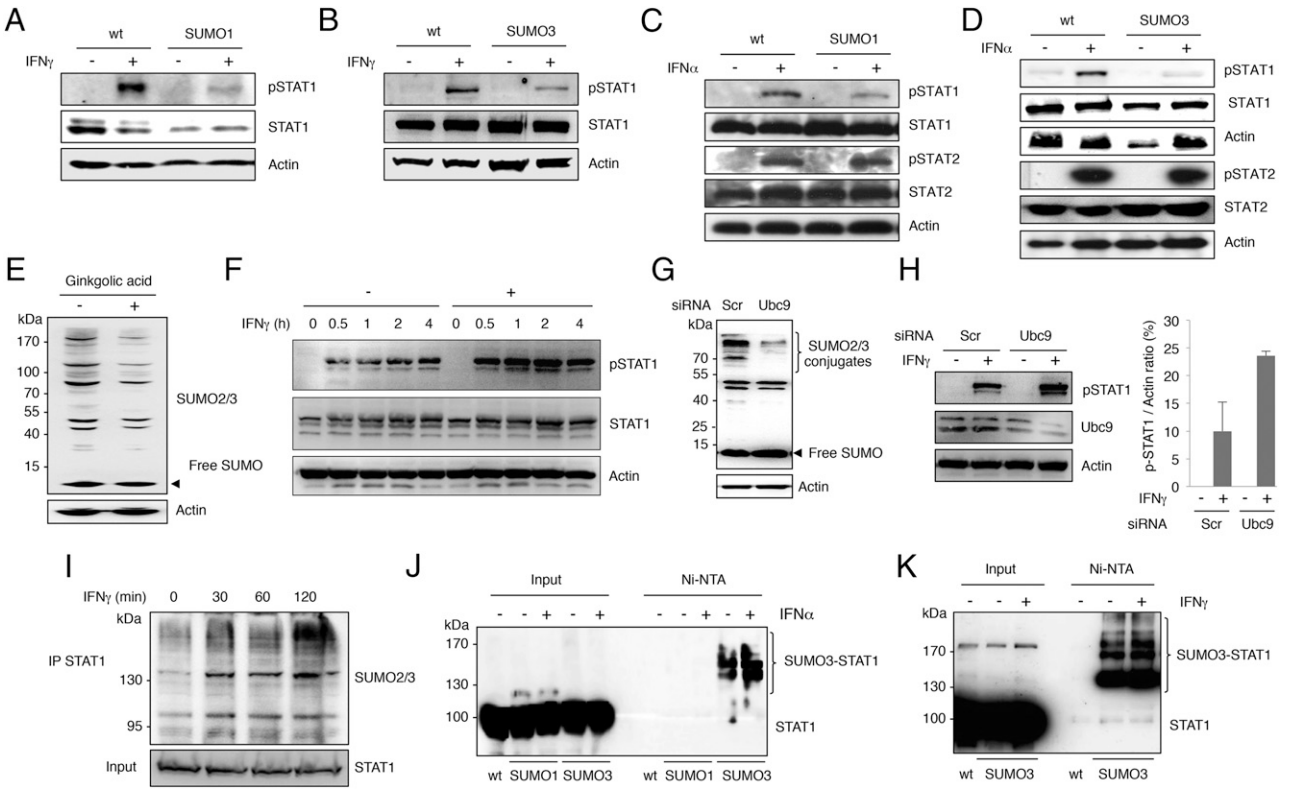

FIGURE 1. Effect of SUMO1 or SUMO3 expression on STAT1 phosphorylation in response to IFN-γ or IFN-α. HeLa-wt, HeLa-SUMO1 (**A** and **C**), or HeLa-SUMO3 (**B** and **D**) cells were treated for 30 min with IFN-γ (A and B) or IFN-α (C and D) at 1000 U/ml. (**E** and **F**) IFN-γ was added for different times to HeLa-wt cells pretreated with 100 μmol ginkgolic acid. In all cases, cells were treated with ginkgolic acid for 6 h. (**G** and **H**) HeLa-wt cells transfected with siRNA scramble (Scr) or siRNA Ubc9 were untreated or treated 2 d later with 1000 U/ml of IFN-γ for 30 min. Equal amounts of cell extracts were analyzed by Western blot for the expression of p-STAT1, p-STAT2, STAT1, STAT2, SUMO2/3, Ubc9, or Actin. P-STAT1/Actin ratios were quantified using Image J software (National Institutes of Health) (H, *right panel*). (**I**) HeLa-wt cells were treated with IFN-γ for the indicated times. Whole-cell lysates were immunoprecipitated with anti-STAT1 Abs and analyzed by SDS-PAGE using anti-SUMO2/3 Abs. HeLa-His-SUMO1 and HeLa-SUMO3 cells were untreated or treated for 30 min with 1000 U/ml of IFN-α (**J**) or IFN-γ (**K**). Cell extracts were purified on Ni-NTA–agarose beads. The inputs and the purified extracts were analyzed by Western blotting using anti-STAT1 Abs.

of the E1-SUMO intermediate (13) or were depleted for Ubc9 (Fig. 1G, 1H), the unique E2-conjugating enzyme for SUMOylation. Both treatments resulted in a decrease in the level of SUMO2/3-modifed proteins (Fig. 1E, 1G) and most notably in a higher level of STAT1 phosphorylation in response to IFN-γ or IFN-α (Fig. 1F, 1H and data not shown).

Because STAT1 is a SUMO substrate, these results prompted us to evaluate the modification of STAT1 by SUMO in cells treated or not with IFN-α or IFN-γ for 30 min. First, we were able to observe an interaction between endogenous STAT1 and endogeneous SUMO2/3 by coimmunoprecipitation. Interestingly, this interaction increased in cells treated 30 min with IFN-γ and reached a maximum at 2 h (Fig. 1I and data not shown). In addition, we found that STAT1 was highly conjugated to SUMO3 in Ni-NTA–purified extracts from untreated HeLa-SUMO3 cells and that treatment with IFN-α (Fig. 1J) or IFN-γ (Fig. 1K) caused an increase of STAT1 conjugation to SUMO3. In contrast, we were not able to detect STAT1 modification by SUMO1 in Ni-NTA–purified extracts from HeLa-SUMO1 cells, although a slower migrating form of STAT1 with an expected size for its conjugation to SUMO1 was detected in the input (Fig. 1J). This latter observation is in line with the notion that SUMO1 conjugation is much more difficult to detect than SUMO2/3 conjugation (14).

Taken together, these results show that stable expression of SUMO results in STAT1 SUMOylation and in a decrease of IFN-induced STAT1 phosphorylation. They also suggest that IFN exerts a negative retrocontrol on its own signaling by increasing STAT1 SUMOylation.

SUMO1 or SUMO3 expression decreases p-STAT1 nuclear localization and DNA binding in response to IFN

Latent STAT1 resides mainly in the cytoplasm of unstimulated cells and undergoes a rapid and transient nuclear accumulation after IFN stimulation (2). In order to analyze the effect of SUMO on IFN-induced STAT1 nuclear accumulation, we first performed indirect immunofluorescence staining to monitor the subcellular distribution of p-STAT1 after stimulation of HeLa-wt, HeLa-SUMO1, and HeLa-SUMO3 cells with IFN.

As anticipated, both IFN-α and IFN-γ promoted an increase in p-STAT1 staining in wt cells (Fig. 2A and 2B). The level of nuclear p-STAT1 staining was much lower when SUMO1 or SUMO3 were overexpressed (Fig. 2A). In line with the absence of effect of SUMO on IFN-α–induced STAT2 phosphorylation, IFN-α promoted a marked increase in nuclear p-STAT2 staining, irrespective of SUMO expression (Fig. 2B).

Next, we investigated the effect of SUMO on the downstream intranuclear step of IFN signaling. In the IFN-γ pathway, p-STAT1 homodimers (called GAF) are translocated to the nucleus, where they bind to a DNA element termed GAS to induce the transcription of ISGs (2). We therefore performed EMSA to analyze the binding capacity of p-STAT1 homodimers to GAS (Fig. 2C). HeLa-wt, HeLa-SUMO1, and HeLa-SUMO3 cells were treated or not with IFN-γ for 30 min, and nuclear extracts were subjected to EMSA with a (α-[^{32}P]) ATP-labeled GAS probe. As expected, upon exposure to IFN-γ, a band corresponding to the slower-migrating product predicted to be a GAF complex was apparent in extracts of HeLa-wt cells (Fig. 2C). The incubation of extracts from IFN-treated HeLa-wt cells with the anti-STAT1 Ab prior to incubation with the probe revealed the presence of a supershifted band, confirming that the GAF complex was composed of the p-STAT1 homodimers (Fig. 2C). In the extracts from HeLa-SUMO1 and HeLa-SUMO3 cells, the amount of GAF complexes was lower, indicating that SUMO overexpression interferes with the IFN-γ–induced DNA binding of p-STAT1 (Fig. 2C).

For the IFN-α–dependent cascade, the transcriptional response relies on the formation of the ISGF3 complex formed by STAT1–STAT2 heterodimers in association with IRF9. Thus, EMSA analysis was performed to analyze the effect of SUMO on the complex formation of ISGF3 with DNA, using an ISRE probe. In nuclear extracts from IFN-α–treated HeLa-wt cells, we observed an increase in ISRE binding activity, which was reversed in the presence of Abs specific for STAT1 and STAT2 (Fig. 2D). Thus, in line with data published previously (15), IFN-α promotes the formation of an ISRE binding complex associating STAT1, STAT2, and IRF9 in wt cells. Quite unexpectedly, nuclear extracts from HeLa-SUMO1 or HeLa-SUMO3 cells treated with IFN-α displayed an ISGF3-like complex ISRE binding activity. The formation of this complex was highly reduced by Abs against STAT2, whereas Abs against STAT1 recognizing the C-terminal region of STAT1 did not (Fig. 2D). To further confirm these results, the EMSA analysis was performed using Abs against STAT1 recognizing either the C- or the N-terminal region of STAT1 (Supplemental Fig. 2). In nuclear extracts from IFN-α–treated HeLa-wt cells, the formation of the ISGF3 complex was reversed in the presence of Abs against STAT1 recognizing either the C- or the N-terminal region of STAT1 (Supplemental Fig. 2). In contrast, none of these anti-STAT1 Abs was able to alter the complex formation in nuclear extracts from IFN-α–treated HeLa-SUMO3 cells (Supplemental Fig. 2). These observations suggest that in SUMO-overexpressing cells, IFN-α mobilizes a STAT1-independent STAT2-containing complex for ISRE binding.

As a whole, our results indicate that stable expression of SUMO1 or SUMO3 decreases IFN-α– and IFN-γ–induced activation and nuclear redistribution of STAT1. This process correlates with lower levels of STAT1 binding to GAS in response to IFN-γ, without altering the binding of an ISGF3-like complex to ISRE in response to IFN-α.

SUMO1 or SUMO3 expression reduces IFN-γ but not IFN-α transcriptional responses

Having shown that SUMO expression alters IFN signaling by reducing IFN-induced STAT1 activation, we next investigated whether SUMO would also affect IFN transcriptional responses. To this purpose, we quantified the activity of ISRE- and GAS-luciferase reporters in HeLa-wt, HeLa-SUMO1, or HeLa-SUMO3 cells in response to IFN-α and IFN-γ, respectively.

As expected, in HeLa-wt cells, IFN-α treatment resulted in a robust induction of ISRE-luciferase reporter gene activity relative to untreated cells (Fig. 3A, *left panel*). Expression of SUMO1 or SUMO3 did not affect IFN-α response transcription, in line with the lack of impact of SUMO expression on the IFN-α–mediated binding of the ISGF3 complex to DNA. Similarly, IFN-γ treatment enhanced GAS-luciferase activity in HeLa-wt cells (Fig. 3A, *right panel*). In this case, the IFN-γ transcriptional response was sensitive to SUMO, with an inhibition of 35 and 85% in cells overexpressing SUMO1 and SUMO3, respectively (Fig. 3A, *right panel*).

Selective effects of SUMO on ISG expression in response to IFN-γ

It was previously shown that a SUMOylation-deficient STAT1 mutant is hyperphosphorylated and has higher DNA binding on STAT1-responsive gene promoters (8, 10, 11), resulting in a selective upregulation of certain IFN-γ–induced ISGs such as *TAP1* (8).

We went to characterize the physiological effect of SUMOylation on some well-characterized IFN-γ–induced genes, such as *IP-10* (also known as *CXCL10*), *TAP1*, *STAT1*, *PKR*, *IRF1*, and *PML* by quantifying their mRNA by quantitative RT-PCR (qRT-PCR) in the

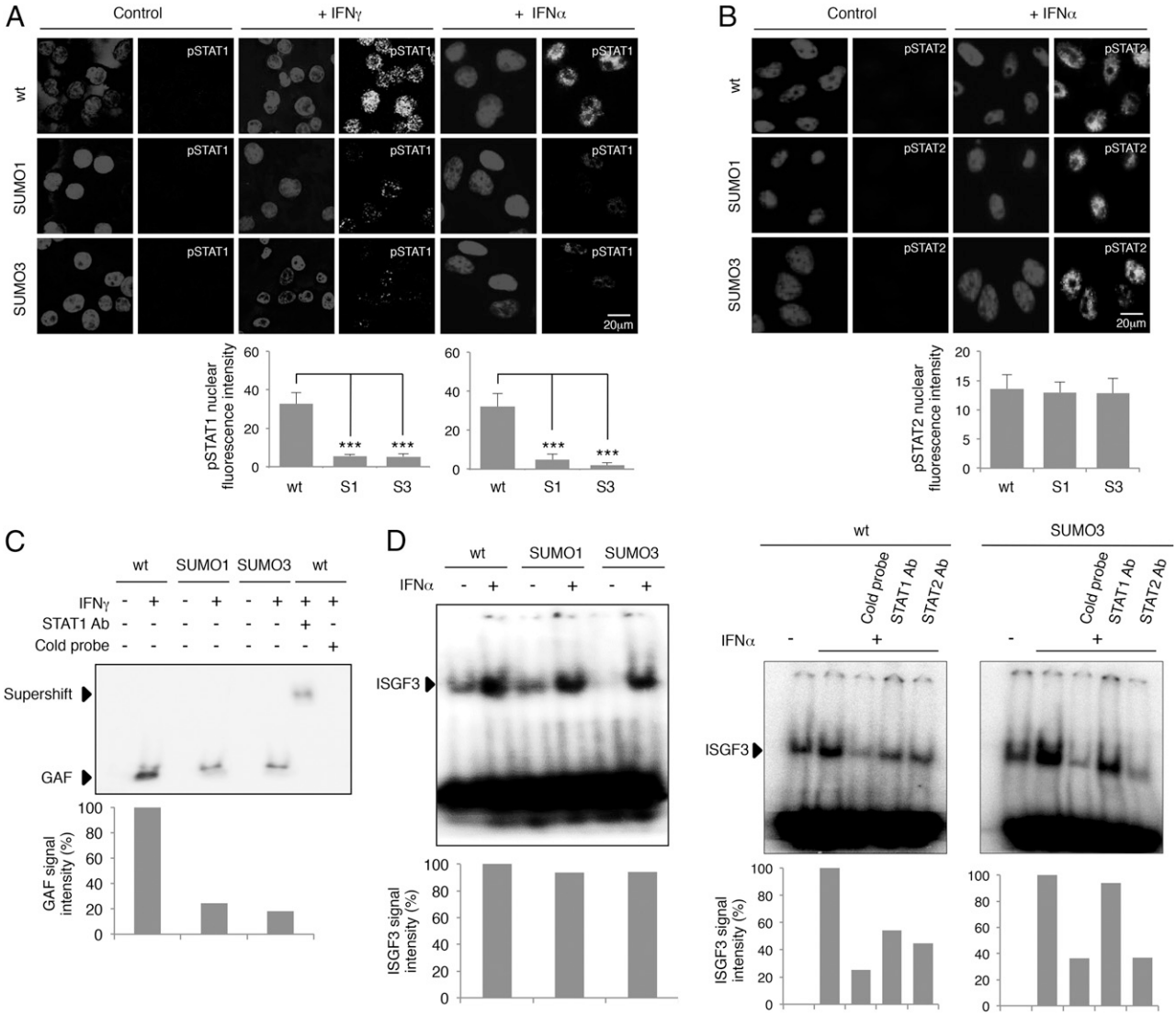

FIGURE 2. Effect of SUMO1 or SUMO3 on STAT1 localization and DNA binding in response to IFN. HeLa-wt, HeLa-SUMO1, and HeLa-SUMO3 cells were treated or not with 1000 U/ml of IFN-γ or IFN-α for 30 min. (**A**) Untreated cells (Control) and cells treated with IFN-γ or IFN-α were stained with anti–p-STAT1 and DAPI. Images obtained in IFN-treated cells were quantified using Image J software (National Institutes of Health). Resulting relative values corresponding to p-STAT1 nuclear fluorescence intensity are shown in histograms below ($n = 10$). Student t test was performed to determine the p value ($^{***}p < 0.001$). (**B**) Untreated cells (Control) or cells treated with IFN-α were stained with p-STAT2 and DAPI. Images obtained in IFN-α–treated cells were quantified using Image J software. Resulting relative values corresponding to p-STAT2 nuclear fluorescence intensity are shown in histograms below ($n = 10$). (**C**) Nuclear extracts of HeLa-wt, HeLa-SUMO1, and HeLa-SUMO3 cells untreated or treated 30 min with IFN-γ were analyzed by EMSA using a GAS α-^{32}P–labeled probe. The specificity of complex formation was confirmed by adding anti-STAT1 Abs or cold probe to the sample. (**D**) Nuclear extracts of HeLa-wt, HeLa-SUMO1, and HeLa-SUMO3 cells untreated or treated with IFN-α for 30 min were examined by EMSA with a ^{32}P–labeled ISRE probe. The specificity of complex formation in the extracts from HeLa-wt and HeLa-SUMO3 cells was confirmed by adding anti-STAT1 or anti-STAT2 Abs to the sample. Quantifications of GAF and ISGF3 signal intensities in the extracts from IFN-treated cells performed using Image J software (National Institutes of Health) are provided below each gel.

extracts from HeLa-wt, HeLa-SUMO1, and HeLa-SUMO3 cells treated with IFN-α or IFN-γ (Fig. 3B). In accord with the literature, the expression of *PML*, *STAT1*, *PKR*, and *TAP1* mRNAs was induced by both IFN-α and IFN-γ, whereas that of *IRF1* and *IP-10* was only sensitive to IFN-γ treatment (Fig. 3B). The upregulation of *PML*, *STAT1*, *PKR*, and *IRF1* mRNA expression induced by IFN-α or IFN-γ was insensitive to SUMO (Fig. 3B). In contrast, SUMO overexpression dramatically reduced the IFN-γ–mediated induction of *IP-10* and *TAP1* mRNA levels (Fig. 3B). These observations are reminiscent of the selective upregulation of particular IFN-γ–induced ISGs, such as the TAP1, which was reported in cells expressing the SUMOylation-deficient STAT1 mutant (8).

Assuming that the differential sensitivity of ISGs to SUMO may relate to differential STAT1 binding affinity to their promoter, we submitted cells to increasing doses of IFN to compare their sensitivity to IFN-dependent induction. For this, HeLa-wt, HeLa-SUMO1, and HeLa-SUMO3 cells were treated or not with IFN-γ or IFN-α for 24 h, and the protein expression of STAT1, PKR, IRF1, IRF9, IP-10, and TAP1 was analyzed by Western blot. These experiments showed that, at low doses of IFN-γ (10 U/ml), STAT1, PKR, and IRF1 proteins were increased, whereas IP-10 and TAP1 proteins can only be detected at higher concentrations of IFN-γ, at 100 and 1000 U/ml, respectively (Fig. 3C). Confirming our qRT-PCR results, the IFN-γ–induced expression of STAT1, PKR, and IRF1 was unaffected by SUMO. In contrast,

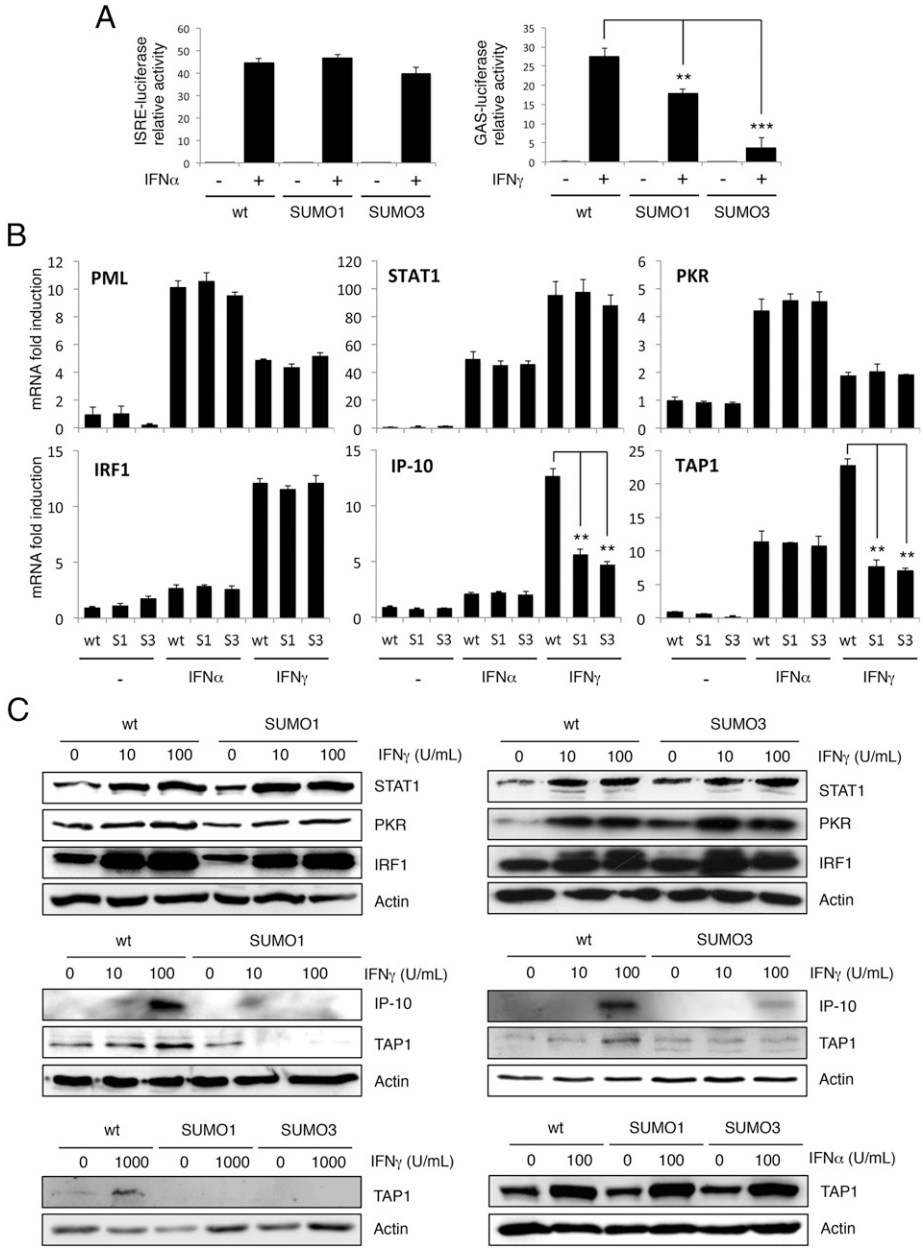

FIGURE 3. Effects of SUMO on IFN transcriptional responses and increase of ISG products. (**A**) HeLa-wt, HeLa-SUMO1, and HeLa-SUMO3 cells were transfected with ISRE-luciferase or GAS-luciferase reporter plasmids. One day posttransfection, cells were left untreated or treated with IFN-α or IFN-γ for 24 h prior to lysis and luciferase assays. (**B**) HeLa-wt, HeLa-SUMO1, and HeLa-SUMO3 cells were untreated or treated with IFN-α or IFN-γ for 8 h. Total RNA was extracted and mRNAs encoding PML, STAT1, PKR, IRF1, IP-10, TAP1, and RPL13A were quantified by qRT-PCR. Means and SDs of three independent experiments are shown. Student *t* test was performed to determine the *p* value. (**C**) HeLa-wt, HeLa-SUMO1, and HeLa-SUMO3 cells were left untreated or treated for 24 h with IFN-α or IFN-γ at the indicated concentrations. Cell extracts were analyzed by Western blot for the expression of STAT1, PKR, IRF1, IP-10, TAP1, or Actin. $^{**}p < 0.01$, $^{***}p < 0.001$.

IP-10 and TAP1 could not be enhanced, even at high concentrations of IFN-γ, when SUMO1 or SUMO3 were overexpressed (Fig. 3C). The inhibition of IFN-induced TAP1 expression by SUMO was specific to the IFN-γ pathways, because IFN-α had comparable effects on TAP1 expression irrespective of SUMO expression (Fig. 3C).

Altogether, these results show that SUMO1 and SUMO3 drastically inhibit the induction of particular ISGs by IFN-γ, whereas the induction of other ISGs is unaffected. The fact that high concentrations of IFN-γ are necessary for inducing IP-10 and TAP1 favors the view that SUMO selectively downregulates the induction of genes requiring high amounts of p-STAT1.

The increase of PML and Sp100 protein expression in response to IFN is impaired by their SUMO3 but not SUMO1 conjugation and subsequent proteasomal degradation

PML is an ISG product required for the formation of PML NBs, which also contain another permanent constituent, the ISG product Sp100 (16–18). We thus assessed the expression of PML and Sp100 and their association with PML NBs in HeLa-wt, HeLa-SUMO1, and HeLa-SUMO3 cells treated or not with IFN-α or IFN-γ for 18 h by Western blot (Fig. 4A, Supplemental Fig. 3A) and immunofluorescence (Supplemental Fig. 3B). As expected, treatment of wt cells with IFN-α or IFN-γ increased the expression of PML and Sp100 proteins, resulting in an increase of the number of PML NBs. This increase was not affected by SUMO1 expression but was impaired by SUMO3 expression (Fig. 4A, Supplemental Fig. 3A, 3B). Because SUMO3 expression abrogated the increase in PML and Sp100 protein expression in response to IFN without altering their mRNA level (Fig. 3B and data not shown), we hypothesized that SUMO3 may promote their degradation. In accord with this hypothesis, increased conjugation of PML to SUMO2/3 was shown to result in its proteasome-dependent degradation (19). To assess the implication of the proteasome pathway, HeLa-wt and HeLa-SUMO3 cells incubated with IFN-γ were left untreated or treated with the proteasome inhibitor MG132 (Fig. 4B, 4C). Treatment with MG132 significantly enhanced PML and Sp100 protein levels in IFN-γ–treated

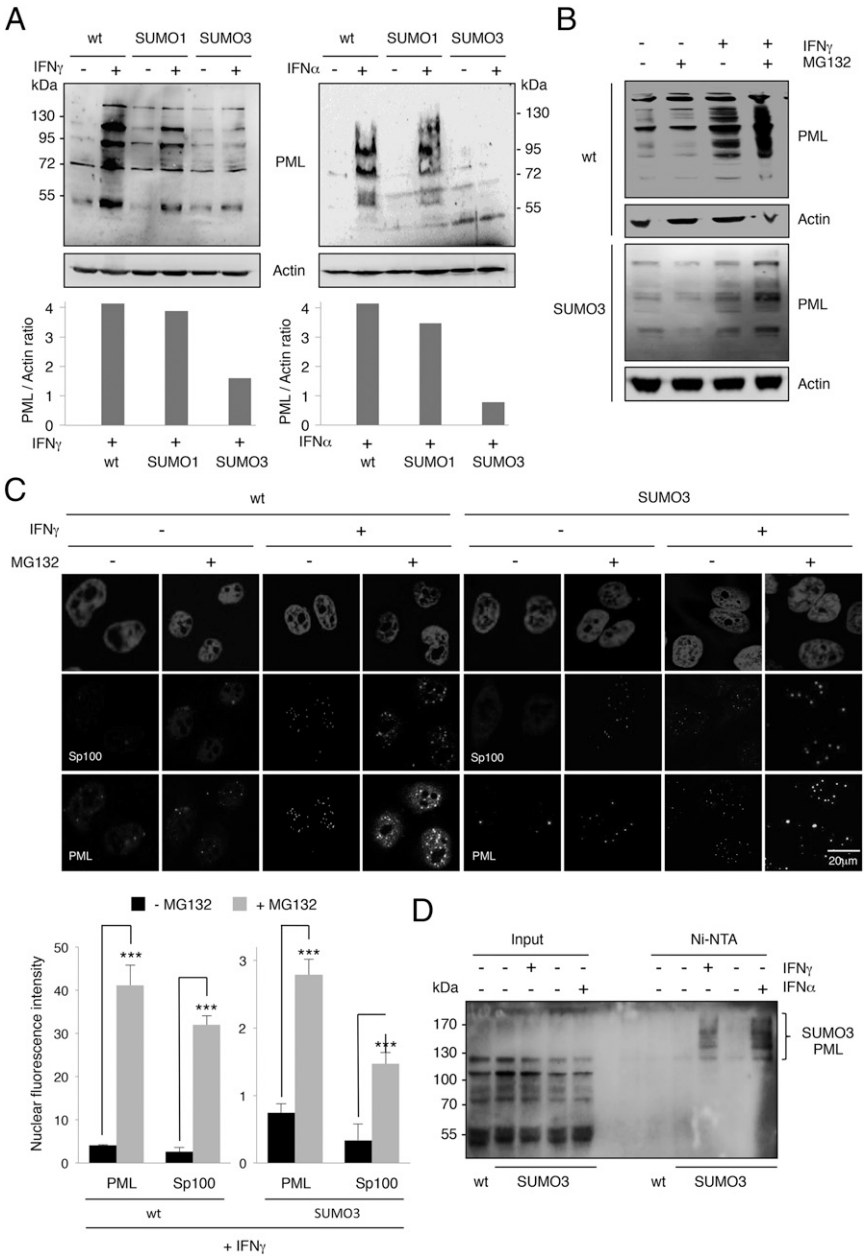

FIGURE 4. IFNs increase PML SUMOylation in SUMO3-expressing cells resulting in its proteasome-dependent degradation. HeLa-wt, HeLa-SUMO1, and HeLa-SUMO3 cells were untreated or treated for 18 h with IFN-α or IFN-γ at 1000 U/ml. (**A**) Cell extracts were analyzed by Western blot for the expression of PML and Actin. PML/Actin ratios were quantified using Image J software (National Institutes of Health). (**B** and **C**) HeLa-wt and HeLa-SUMO3 cells were untreated or treated with 1000 U/ml of IFN-γ in the presence or not of 10 μmol of MG132. Cell extracts were analyzed by immunoblot for PML and Actin (B), and immunofluorescence analysis was performed for PML and Sp100 staining (C). Relative values corresponding to PML and Sp100 nuclear fluorescence intensity in cells treated with IFN-γ in the absence or the presence MG132 are shown in histograms ($n = 10$) (C, *bottom panel*). Student t test was performed to determine the p value (***$p < 0.001$). (**D**) HeLa-SUMO3 cells were untreated or treated for 30 min with 1000 U/ml of IFN-α or IFN-γ. Cell extracts were purified on Ni-NTA–agarose beads. The inputs and purified extracts were analyzed by Western blotting using anti-PML Abs.

wt cells, as revealed by Western blot (Fig. 4B and data not shown) and double immunofluorescence (Fig. 4C). Interestingly, in SUMO3-overexpressing cells, MG132 treatment restored the capacity of IFN-γ to enhance PML and Sp100 protein expression, due to the abrogation of their SUMO3-induced degradation. Thus, we can conclude that SUMO3 targets these two ISG products for proteasomal degradation in IFN-treated cells.

We next asked whether this proteosomal degradation depends on the increased conjugation of PML or Sp100 to SUMO3. Therefore, we evaluated the capacity of IFN in SUMO3-expressing cells to enhance SUMOylation of endogenous PML and Sp100 proteins. To do this, HeLa-SUMO3 cells were left untreated or treated with IFN-α or IFN-γ for 30 min. Cell extracts purified on Ni-NTA–agarose beads and analyzed by immunoblot revealed that both IFNs increased PML and Sp100 conjugation to SUMO3 (Fig. 4D, Supplemental Fig. 3C).

Our results show that in SUMO3-expressing cells, treatment with IFN-α or IFN-γ results in a rapid and high increase of PML and Sp100 SUMOylation that is followed by their proteasomal degradation. Therefore, SUMO3 expression impairs the capacity of IFN to enhance PML and Sp100 proteins, resulting in a loss of PML NBs.

RNF4 depletion stabilizes PML, leading to positive regulation of IFN-γ signaling and transcriptional response

SUMO2/3 can act as a signal for the recruitment of RNF4, which acts as a SUMO-dependent E3 ubiquitin-ligase (19). RNF4 binding to SUMO2/3-modified PML leads to its ubiquitination and subsequent degradation upon cell treatment with arsenic trioxide (As_2O_3) (19, 20). RNF4 preferentially degrades SUMO2/3-modified PML as compared with SUMO1-PML (19). We therefore tested whether downregulation of RNF4 by RNA interference could stabilize PML protein expression in IFN-treated HeLa-wt and HeLa-SUMO3 cells. Depletion of RNF4 in HeLa-wt cells (Fig. 5A) resulted in a marked enhancement of PML protein expression in untreated and IFN-treated cells compared with untransfected cells or cells transfected with a scramble siRNA (Fig. 5B, *top panel*). Similarly, RNF4 depletion in IFN-treated

HeLa-SUMO3 cells (Fig. 5A) prevented PML degradation (Fig. 5B, *bottom panel*), thus restoring an increase of PML protein expression in response to IFN.

In a previous work, we have shown that expression of all nuclear PML isoforms induces a higher IFN-γ–induced STAT1 activation and transcriptional response (21). Thus, our prediction was that the stabilization of IFN-induced PML by RNF4 depletion would reinforce IFN-γ signaling and transcription. Indeed, as shown in Fig. 5C, stabilization of PML in HeLa-wt cells by RNF4 knockdown led to enhanced STAT1 phosphorylation in response to IFN-γ, itself resulting in an increase of IFN-γ transcriptional response (Fig. 5D). In contrast, depletion of RNF4 (Fig. 5D) resulted in a higher IFN-α–induced STAT1 phosphorylation but did not alter the transcriptional response to IFN-α. Thus, the stabilization of PML allowed by the downregulation of RNF4 is correlated with a positive regulation of IFN-γ signaling and transcriptional response.

In Fig. 3A, we showed that SUMO1 and SUMO3 expression in HeLa cells resulted in ∼35 and 85% inhibition of IFN-γ transcriptional response, respectively. Because PML protein expression was not increased in IFN-treated HeLa-SUMO3 cells due to its degradation (Fig. 4B), we suspected that this lack of PML would contribute to the higher inhibitory effect of SUMO3 on IFN-γ–induced transcription. To test this hypothesis, we quantified the transcriptional response of the GAS-luciferase reporter construct after depletion of RNF4 or PML in HeLa-wt, HeLa-SUMO1, and HeLa-SUMO3 cells treated with IFN-γ (Fig. 5E). In this experiment, we observed two different levels of inhibition: one intermediate, between 30 and 50% (gray), and a nearly complete inhibition of ∼80–90% (black). These two phenotypes illustrate the dual effect of SUMO paralogs on IFN-γ signaling, by acting both on STAT1 phosphorylation and PML stability. In wt cells transfected with the scramble siRNA, IFN-γ–induced luciferase transcription was arbitrary set to 100%. As previously reported (21), PML downregulation in wt cells partly reduced IFN-γ response transcription (gray) (Fig. 5E). In SUMO1-expressing cells, IFN-γ–induced transcription was inhibited (gray), and this inhibition was amplified when PML expression was depleted

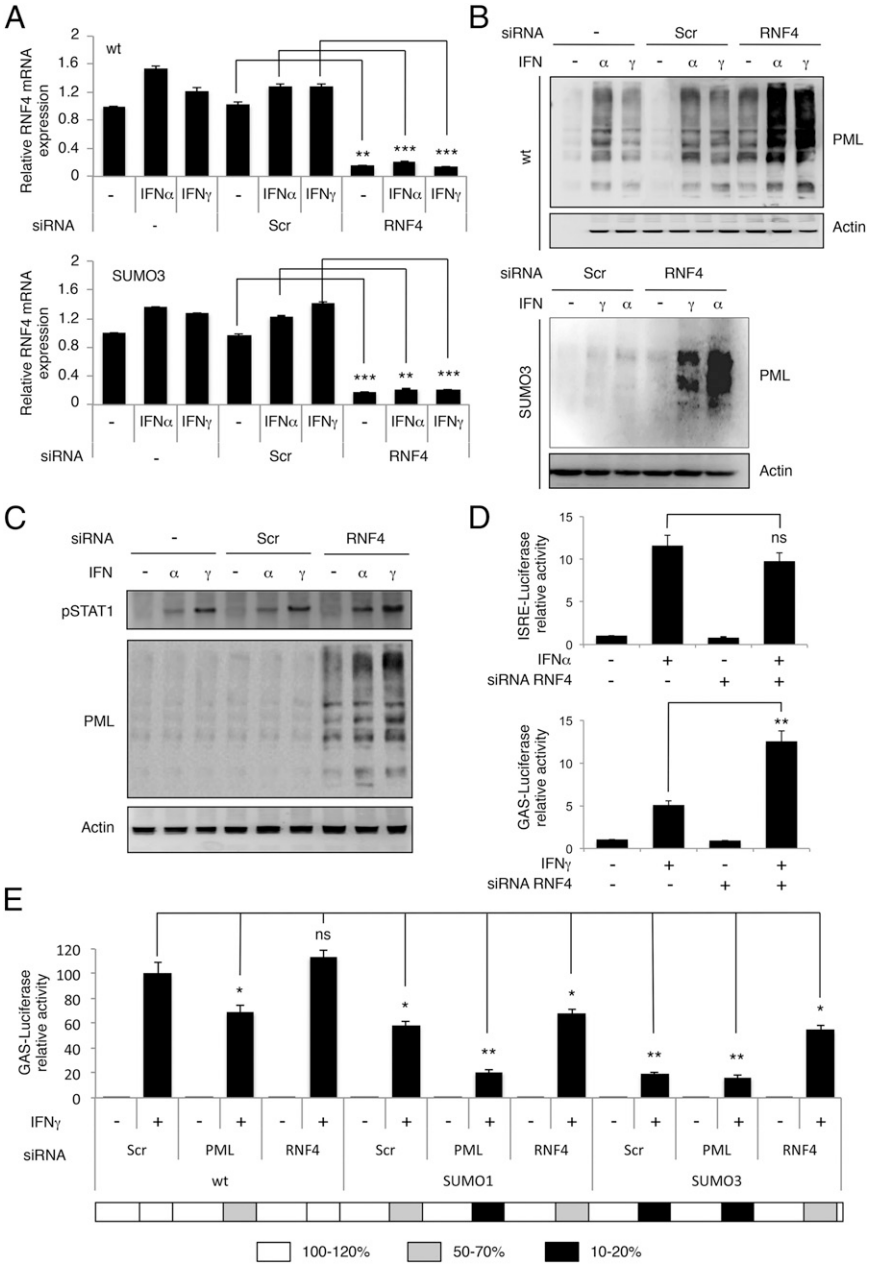

FIGURE 5. Depletion of RNF4 stabilizes PML isoforms and enhances IFN-γ–induced STAT1 activation and transcription. (**A** and **B**) HeLa-wt and HeLa-SUMO3 cells were transfected with RNF4-specific siRNA or scrambled (Scr) siRNA. One day posttransfection, cells were treated with 1000 U/ml of IFN-α or IFN-γ for 24 h. (A) Knockdown efficiency of RNF4 was estimated by qRT-PCR in HeLa-wt (*top panel*) and HeLa-SUMO3 (*bottom panel*) cells. (B) Western blot analysis was performed for PML and Actin expression in extracts from HeLa-wt (*top panel*) and HeLa-SUMO3 (*bottom panel*) cells. (**C**) HeLa-wt cells were transfected with RNF4-specific siRNA or Scr siRNA. One day posttransfection, cells were treated with 1000 U/ml of IFN-α or IFN-γ for 30 min. Western blot analysis was performed for PML, p-STAT1, and Actin expression. (**D**) HeLa-wt cells were transfected with ISRE-luciferase or GAS-luciferase reporter plasmids and either Scr siRNA or RNF4-specific siRNA. One day posttransfection, cells were treated or not with 1000 U/ml of IFN-α or IFN-γ for 24 h prior to lysis and luciferase assays. (**E**) HeLa-wt, HeLa-SUMO1, or HeLa-SUMO3 cells were transfected with GAS-luciferase reporter plasmid and Scr siRNA, RNF4-specific siRNA, or PML-specific siRNA. One day posttransfection, cells were treated or not with 1000 U/ml of IFN-γ for 24 h prior to lysis and luciferase assays. Results are represented as the percentage of Luciferase activity compared with cells transfected with Scr siRNA and treated with IFN-γ that was arbitrarily set to 100%. Underneath the graph are illustrated the 3 phenotypes obtained, which are represented as a color code corresponding to the percentage of residual Luciferase activity. All data were analyzed by Student *t* test. $*p < 0.05$, $**p < 0.01$, $***p < 0.001$.

(black). Finally, in cells overexpressing SUMO3, the inhibition of GAS-driven transcription in response to IFN-γ was nearly complete (black), because it resulted from a 2-fold effect of SUMO3: the inhibition of STAT1 phosphorylation combined to PML degradation. In agreement, PML depletion by siRNA in SUMO3-expressing cells did not lead to further inhibition. In contrast, RNF4 downregulation, which prevents PML degradation, led to a partial recovery of IFN-γ transcriptional response (gray) (Fig. 5E).

Altogether, these results show that both SUMO1 and SUMO3 inhibit IFN-γ transcriptional response and that this inhibition could be further amplified in SUMO3-expressing cells due to PML degradation.

SUMO1 and SUMO3 impair IFN-induced biological responses

Finally, we sought to evaluate the role of SUMO on IFN-induced biological activities. We analyzed the capacity of IFN-α and IFN-γ to inhibit EMCV production in wt cells and in cells stably expressing SUMO1 or SUMO3. To test whether SUMO alters the antiviral effect of IFN, it is important to infect cells with a virus for which replication is not impaired by SUMO alone. Note that SUMO1 or SUMO3 expression did not alter EMCV protein expression and EMCV production in the absence of IFN treatment (Fig. 6A), which is not the case for other viruses such as vesicular stomatitis virus or HSV-1 (data not shown). Cells were treated with 100 U/ml of IFN-α or IFN-γ for 24 h prior to infection with EMCV at an MOI of 5 for 8 h (Fig. 6A). Cell extracts were analyzed by Western blot, and viral titers were determined by measuring the $TCID_{50}$. After IFN-α or IFN-γ treatment, EMCV proteins were no longer detectable in HeLa-wt or HeLa-SUMO1 cells. In contrast, SUMO3 overexpression reduced the capacity of IFN-α and IFN-γ to inhibit viral proteins and EMCV production (Fig. 6A). These results are consistent with the degradation of PML in IFN-treated HeLa-SUMO3 cells (Fig. 4A) and with our previous observation that PML depletion decreases the anti-EMCV effect of IFN (12).

Next, to obtain a more complete picture of the biological consequences of SUMOylation, we investigated another well-defined

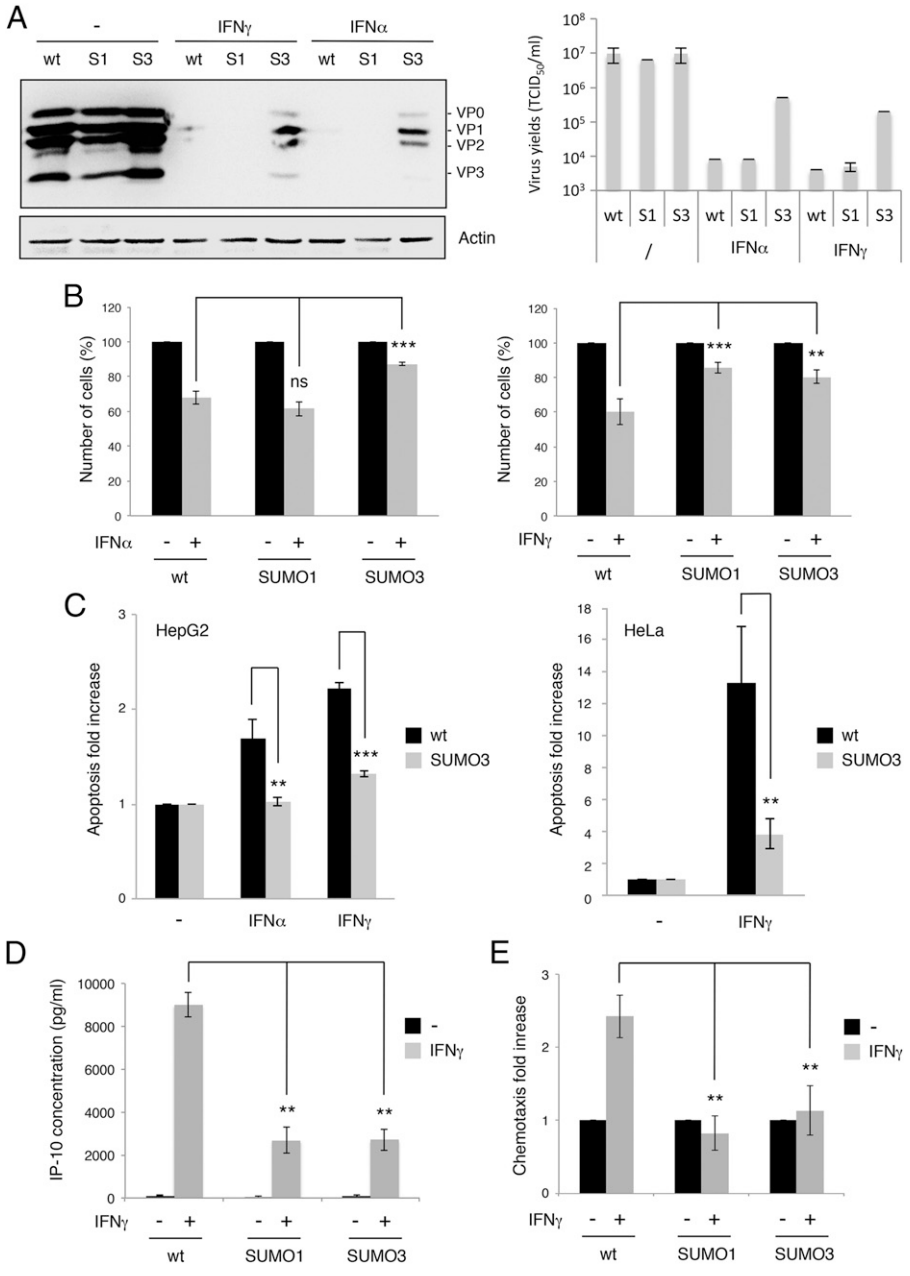

FIGURE 6. Effects of SUMO on IFN-induced biological responses. (**A**) Effects of SUMO on IFN-induced anti-EMCV activity. HeLa-wt cells and cells stably expressing SUMO1 (S1) or SUMO3 (S3) were treated with 100 U/ml of IFN-α or IFN-γ for 24 h then infected with EMCV at an MOI of 5 for 8 h. Cell extracts were analyzed for viral proteins and Actin (*left panel*), and culture supernatants were used for the determination of viral titers by measuring the $TCID_{50}$ (*right panel*). (**B**) HeLa-wt, HeLa-SUMO1, or HeLa-SUMO3 cells were treated or not with 1000 U/ml of IFN-α or IFN-γ. The number of viable cells after 4 d was estimated using an MTT assay. Results are presented as the percentage of cells in IFN-treated cells compared with untreated cells that was arbitrary set to 100%. (**C**) Effects of SUMO on IFN-induced apoptosis. HepG2 and HeLa wt cells or expressing SUMO3 were treated with 1000 U/ml of IFN-α or IFN-γ for 3 d. The proportion of apoptotic cells stained with FITC labeled Annexin V and PI was estimated by FACS. Results are expressed as the ratio of apoptotic cells in IFN-treated cells compared with untreated cells that was arbitrary set to 1. (**D**) HeLa-wt, HeLa-SUMO1, or HeLa-SUMO3 cells were treated or not with 1000 U/ml of IFN-γ for 3 d, and the amount of IP-10 secreted in the medium was quantified by ELISA. (**E**) HeLa-wt, HeLa-SUMO1, or HeLa-SUMO3 cells cultivated in the bottom chamber of a transwell plate were left untreated or treated with 1000 U/ml of IFN-γ. Seventy-two hours later, 5×10^5 activated human T lymphocytes was added in the upper chamber. After 8 h, the number of T cells that migrated to the lower chamber was determined by flow cytometry. All data were analyzed by Student *t* test. $^{**}p < 0.01$, $^{***}p < 0.001$.

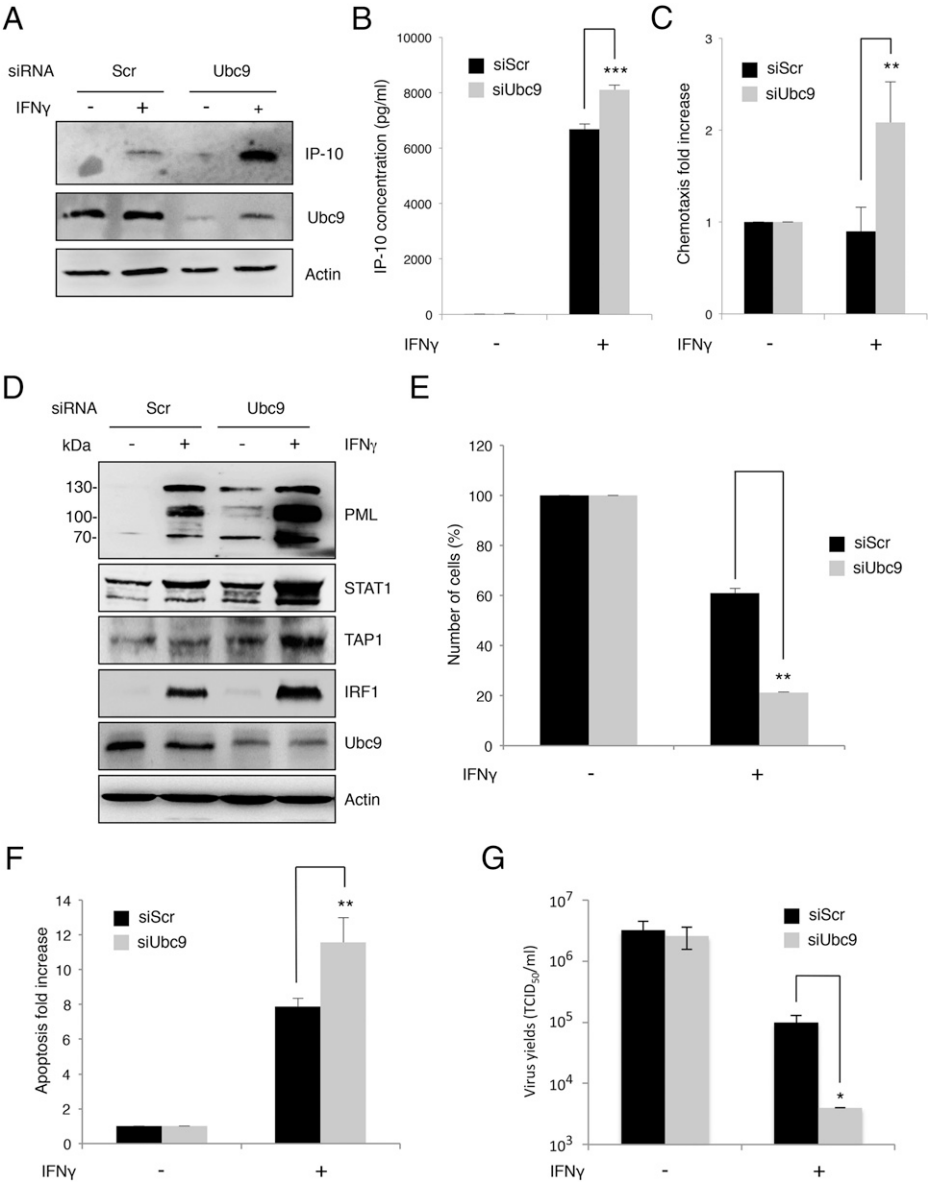

FIGURE 7. Ubc9 depletion in wt cells increases IFN-γ–induced ISG products and biological response. (**A**) Western blot for IP10 and Ubc9 expression in wt-cells depleted for Ubc9 and treated with 100 U/ml of IFN-γ for 24 h. (**B**) The same experiment was performed as in Fig. 6D in wt-cells depleted for Ubc9 and treated with 100 U/ml of IFN-γ for 3 d. (**C**) The same experiment was performed as in Fig. 6E in wt-cells depleted for Ubc9 and treated with 100 U/ml of IFN-γ for 3 d. (**D**) Extracts from wt-cells depleted for Ubc9 and treated with 100 U/ml of IFN-γ were analyzed by Western blot for PML, STAT1, TAP1, IRF1, Ubc9, and Actin expression. (**E**) HeLa-wt transfected with siRNA scramble (siScr) or siRNA Ubc9 (siUbc9) were treated or not with 100 U/ml of IFN-γ. The number of viable cells after 4 d was estimated using an MTT assay. Results are presented as the percentage of cells in IFN-γ–treated cells compared with untreated cells that was arbitrary set to 100%. (**F**) Cells were treated as in (**E**) for 3 d. The proportion of apoptotic cells stained with FITC-labeled Annexin V and PI was estimated by FACS. Results are expressed as the ratio of apoptotic cells in IFN-treated cells compared with untreated cells that was arbitrary set to 1. (**G**) HeLa-wt transfected with siRNA Scr or siRNA Ubc9 were treated or not with 10 U/ml of IFN-γ for 20 h before infection with EMCV at an MOI of 5 for 8 h. Culture supernatants were used for the determination of viral titers by measuring the $TCID_{50}$ (*right panel*). All data were analyzed by Student *t* test. $*p < 0.05$, $**p < 0.01$, $***p < 0.001$.

property of IFNs, which is their antiproliferative/proapoptotic activity. HeLa-wt, HeLa-SUMO1, and HeLa-SUMO3 cells were grown for 4 d in the presence of 1000 U/ml of IFN-α or IFN-γ, and the number of living cells was estimated by an MTT assay. As shown in Fig. 6B, in wt cells, IFN-α induced a reduction of cell proliferation of ~30%. A similar 30% reduction in cell proliferation was monitored in HeLa-SUMO1 cells, whereas SUMO3 overexpression rescued cell proliferation to ~100% (Fig. 6B). Because neither SUMO1 nor SUMO3 affect IFN-α transcriptional response, whereas SUMO3 (but not SUMO1) promotes PML degradation, this selective effect of SUMO3 is probably the consequence of the proteasome-dependent degradation of PML, which is a well-known tumor suppressor. In contrast, both SUMO1 and SUMO3 expression attenuated the antiproliferative effect of IFN-γ (Fig. 6B), further confirming that inhibition of IFN-γ signaling by SUMO paralogs had biological consequences. Next, we went on to investigate the consequences of SUMO3 expression on IFN-α–induced apoptosis in the hepatoma cell line HepG2. Indeed, IFN-α–induced apoptosis in HepG2 cells is known to involve PML (22), and our above data show that PML protein expression is not enhanced by IFN in cells expressing SUMO3. HepG2 cells expressing SUMO3-YFP were treated for 3 d with 1000 U/ml IFN-α or IFN-γ, and the proportion of apoptotic cells was estimated by flow cytometry using Annexin V/PI staining on both SUMO3-YFP–negative and SUMO3-YFP–positive subpopulations (Fig. 6C, *left panel*). The results show that SUMO3 expression reduced the rate of apoptosis in HepG2 cells treated either with IFN-α or IFN-γ. This further confirms that SUMO3 blocked IFN response via PML degradation. Furthermore, IFN-γ–induced apoptosis was also inhibited by SUMO3 expression in HeLa cells (Fig. 6C, *right panel*), suggesting that PML may also be involved, although the involvement of other ISG products cannot be ruled out.

Finally, we assessed the biological consequences of the specific inhibition of the IFN-γ–mediated induction of defined ISGs by SUMO3. We focused on IP-10, for which IFN-γ–induced expression was particularly affected (Fig. 3B, 3C). We first compared the amount of IP-10 secreted in response to IFN-γ by HeLa-wt, HeLa-SUMO1, or HeLa-SUMO3 cells through ELISA. In line with our qRT-PCR (Fig. 3B) and Western blot (Fig. 3D) data, both SUMO1 and SUMO3 expression led to a dramatic decrease of IP-10 secretion in response to IFN-γ (Fig. 6D). IP-10 is also known as CXCL10 and is able to attract monocytes/macrophages, T cells, NK cells, and dendritic cells (23). Thus, we tested the effect of SUMO

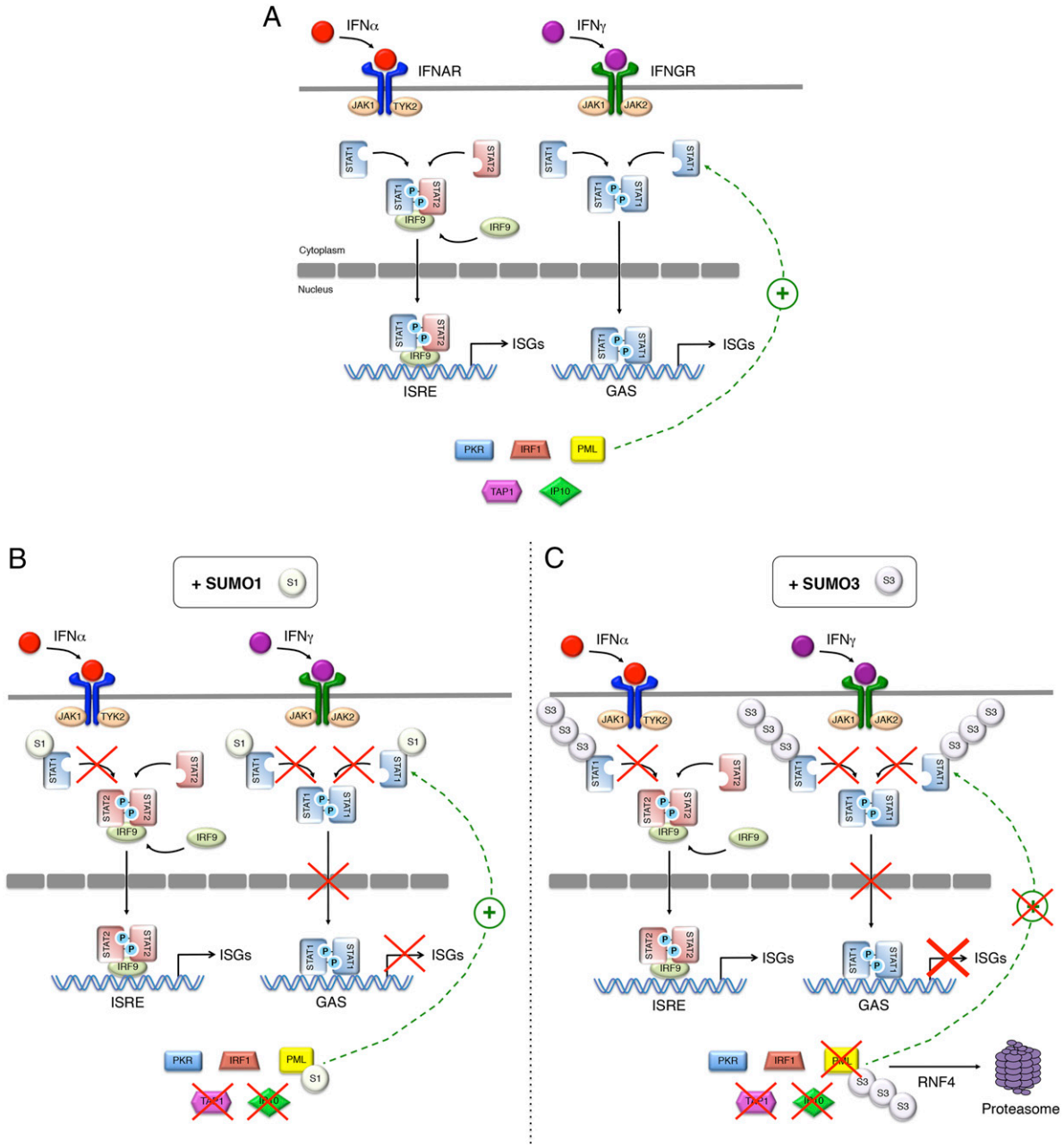

FIGURE 8. Model for SUMO1- and SUMO2/3-mediated inhibition of IFN signaling. (**A**) The interaction of IFN-α with IFNAR leads to the activation of the JAK tyrosine kinases (Tyk2 and JAK1) that phosphorylate STAT1 and STAT2. p-STAT1 and p-STAT2 heterodimerize and translocate into the nucleus to induce ISGs harboring an ISRE. The binding of IFN-γ to its receptor, IFNGR, results in the phosphorylation of STAT1 by JAK1 and JAK2. p-STAT1 homodimers migrate to the nucleus and bind to a DNA element termed GAS in the promoter of specific ISGs such as IRF-1, TAP1, IP-10, Sp100, and PML. In return, PML positively regulates IFN-γ signaling (21). (**B**) SUMO1 overexpression leads to an inhibition of STAT1 phosphorylation in response to IFN. Whereas the IFN-α transduction pathway is unaffected by this inhibition, because STAT2 homodimers can compensate the lack of STAT1 phosphorylation, the IFN-γ transduction pathway is impaired, as illustrated by the reduced capacity of STAT1 to bind GAS. This leads to a dramatic decrease of the expression of certain IFN-γ–induced genes, such as TAP1 and IP-10. The inhibition of IFN-γ transduction pathway is partly compensated by PML, for which modification by SUMO1 does not reduce its activity. (**C**) In response to IFN, SUMO3 overexpression also leads to an inhibition of STAT1 phosphorylation and binding to GAS resulting in an inhibition of TAP1 and IP-10 mRNA expression. In addition, IFN-induced PML modification by poly-SUMO3 chains leads to its RNF4-dependent ubiquitination and its subsequent degradation by the proteasome. Thus, the effect of hyper-SUMOylation by SUMO3 leads to a more pronounced phenotype, because PML cannot exert its positive activity on IFN-γ signaling due to its proteasomal degradation.

on chemotaxis using activated human T lymphocytes. As shown in Fig. 6E, expression of SUMO1 or SUMO3 abrogated the capacity of IFN-γ to promote T cell chemoattraction. Although we cannot rule out the involvement of other chemokines, this result illustrates the fact that the inhibition of IFN-γ–induced expression of IP-10 by SUMO paralogs correlates with the inhibition of chemotaxis. To further confirm these results, we depleted Ubc9 in wt cells. As shown in Fig. 1H, Ubc9 depletion enhanced IFN-γ–induced STAT1 phosphorylation and also IFN-γ–induced IP10 expression (Fig. 7A) and secretion (Fig. 7B), which are correlated with a significant increase of chemotaxis (Fig. 7C). In addition, Ubc9 depletion in IFN-γ–treated cells enhanced the induction of ISG products such as PML, IRF1, TAP1, and STAT1 (Fig. 7D), the anti–cell growth effect (Fig. 7E), the induction of apoptosis (Fig. 7F), and the inhibition of

EMCV production (Fig. 7G). Therefore, our results show that inhibition of SUMOylation results in a higher IFN-γ–induced STAT1 phosphorylation that is correlated with enhanced biological responses. Our results are summarized in an illustration depicting SUMO1 and SUMO2/3-mediated inhibition of IFN signaling (Fig. 8).

Discussion

In this study, we report that SUMO1 and SUMO3 selectively impair IFN-γ signaling by inhibiting STAT1 phosphorylation and therefore downstream events. Also, we show that IFN exerts a negative retrocontrol on its own signaling by enhancing STAT1 SUMOylation. Furthermore, we found that SUMO3, but not SUMO1, further inhibits IFN-γ transcriptional response through SUMO3-dependent PML degradation.

First, we showed that the stable expression of SUMO1 or SUMO3 in different human cell lines alters IFN-γ action at the level of signaling and transcription of ISGs. Indeed, SUMO1 or SUMO3 overexpression led to a lower STAT1 phosphorylation. At the opposite, inhibition of SUMOylation in wt cells treated with ginkgolic acid or depleted for Ubc9 resulted in an increased IFN-γ–induced STAT1 activation. It was found that STAT1 is conjugated to SUMO1 on K703 and that the corresponding mutant exhibits a higher transcriptional activity than the wt protein (8, 9). However, the physiologic function of STAT1 SUMOylation on IFN responses was not evaluated. In this study, we demonstrated that stable expression of SUMO1 or SUMO3 in human cells reduced GAS-luciferase activity in response to IFN-γ, whereas quantitative qRT-PCR revealed a selective reduction of STAT1-mediated ISG mRNA expression. Indeed, expression of SUMO1 or SUMO3 reduced IFN-γ–induced mRNA expression of IP-10 and TAP1 but did not affect mRNA levels of IRF1, PKR, STAT1, and PML. We were able to confirm these observations at the protein level because IFN-γ did not increase TAP1 and IP-10 protein expression in SUMO1- or SUMO3-expressing cells. This inhibition has biological consequences, because we found that SUMO overexpression causes a dramatic reduction of IP-10–induced chemotaxis and that opposite results were obtained in wt cells depleted for Ubc9.

In wt cells, whereas IRF1, STAT1, or PKR were increased at low doses of IFN-γ (10 U/ml), the increase of IP-10 and TAP1 expression required higher concentrations of IFN-γ. This suggests that the ISGs that are induced by low doses of IFN are not affected by the expression of SUMO, whereas those induced by high doses are affected, probably due to the fact that there is less available activated STAT1. Such a selective inhibition of the induction of certain ISGs by SUMO has previously been observed, because the expression of a SUMOylation-deficient STAT1 mutant resulted in the selective increase of CBP1 and TAP1 expression, whereas other ISGs such as IRF1 were not affected (8).

In addition, we showed that although overexpression of SUMO1 or SUMO3 decreased STAT1 activation in response to IFN-α, it did not alter STAT2 phosphorylation, binding of ISGF3 to the ISRE, or transcriptional response. Type I IFN signaling is a complex process, as they can activate several kinases in addition to JAKs, other STATs in addition to STAT1 and STAT2, and even other transcription factors (24–26). In addition, accumulating evidence supports the existence of alternative STAT2 signaling pathways that are independent from STAT1 (27). Indeed, in response to IFN-α, STAT2 was shown to form, independently from STAT1, a complex with IRF9 (28) that binds ISRE and mediates ISG expression (29). Also, it was shown that whereas STAT1 cooperativity is essential for IFN-γ response, it is dispensable for IFN-α signaling (30). Very recently, it has been reported that IFN-α activates the STAT2/IRF9 complex that forms an ISGF3-like response without STAT1 and generates an antiviral response in the absence of STAT1 (31). Accordingly, in our report, we show that although SUMO decreased STAT1 phosphorylation in response to IFN-α, it did not alter the formation of ISGF3-like complex and the transcriptional response. Therefore, it is likely that SUMO overexpression has no effect on IFN-α signaling, because alternative complexes, such as p-STAT2 homodimers (Fig. 8), can compensate the reduction of STAT1 phosphorylation.

PML and Sp100 proteins are the major permanent constituents of PML NBs and are ISG products (16–18). It is established that PML is modified by SUMO under normal growth conditions (32, 33) and that As_2O_3 enhances PML SUMOylation and promotes its interaction with RNF4, a poly–SUMO-dependent ubiquitin E3 ligase responsible for proteasome-mediated PML degradation (19, 20). We demonstrated in this report that in SUMO3-expressing cells, IFN-α and IFN-γ increased PML and Sp100 SUMOylation (Fig. 4), induced their mRNA (Fig. 3B and data not shown) without enhancing their protein level due to their proteosomal degradation (Fig. 4), and thus cancelled the IFN-mediated increase in PML and Sp100 protein expression (Fig. 8). Accordingly, treatment of SUMO3-expressing cells with the proteasome inhibitor (Fig. 4B) or depletion of RNF4 (Fig. 5B) restored the increase of PML proteins in response to IFN-α and IFN-γ. It should be noted that the endogenous level of PML is similar in wt cells or cells expressing SUMO3 (Fig.3A), demonstrating that SUMO3 expression alone did not alter PML protein level. We cannot rule out that targets for IFN-induced SUMOylation and degradation in SUMO3-overexpressing cells may include proteins distinct from PML and Sp100. However, IFNs can enhance protein SUMOylation without resulting in their downregulation because we showed that IFNs enhanced STAT1 SUMOylation in SUMO3-expressing cells without altering its protein level (Fig. 3C).

In line with the selective effect of SUMO3, whereas SUMO1 expression induced a modest reduction of IFN-γ transcriptional response of ~35%, this reduction reached 85% with SUMO3. We were able to demonstrate that the higher inhibition of ISG transcription in response to IFN-γ in SUMO3- versus SUMO1-expressing cells results from the enhanced degradation of PML. Accordingly, stabilization of PML by RNF4 depletion in HeLa-wt cells results in an increase of IFN-γ–induced STAT1 phosphorylation and transcriptional responses. Also, depletion of RNF4 reduced the inhibitory effect of SUMO3 on IFN-γ transcriptional response (Fig. 8). These results recall our previous report, showing that PML positively regulates IFN-γ signaling resulting in an increased induction of ISGs (21).

It is now well established that PML plays an important role in antiviral defense and IFN response (34–36). In this study, we report that PML degradation correlates with a decrease in IFN-induced antiviral state. Indeed, in SUMO3-expressing cells, the IFN-induced increase in PML expression is impaired, resulting in a decrease of IFN-induced anti-EMCV activity. These observations perfectly fit with our previous report that PML depletion in human cells boosts EMCV production and reduced the capacity of IFN to protect them from EMCV infection (12).

In addition to IP-10–induced chemotaxis and PML-mediated EMCV protection, our data shed light on the consequences of SUMO expression on the antiproliferative and proapoptotic effect of IFN. Whereas only SUMO3 counteracts the antiproliferative activity of IFN-α, probably due to PML degradation, both SUMO1 and SUMO3 could rescue cell proliferation induced by IFN-γ. Finally, we showed that in HepG2 cells, in which IFN-induced apoptosis is known to depend on PML, SUMO3 expression was able to reduce the apoptotic process. More surprisingly,

we found that SUMO3 could also rescue HeLa cells from IFN-γ–induced apoptosis, suggesting either that PML is also implicated or that other ISG products can be affected by SUMO3 overexpression.

Taken together, our results uncover an unprecedented role of SUMOylation in attenuating cell sensitivity to IFN-γ by decreasing STAT1 activation, its binding to DNA, and the transcription of specific ISGs. Conversely, inhibition of SUMOylation resulted in a higher IFN-γ–induced STAT1 phosphorylation and enhanced biological responses. Also, we show that by IFN exerts a negative retrocontrol on its own signaling by enhancing STAT1 SUMOylation. Furthermore, we provide evidence for a specific action of SUMO3, which abrogates the increase of NB-associated PML and Sp100 protein expression in response to type I and II IFNs by inducing their proteasome-mediated degradation. We cannot exclude that SUMOylation may alter other factors involved in signaling, transcription, or protein stability. It will be interesting to identify which proteins are conjugated to SUMO in response to IFN in future studies. As a conclusion, our work allows including SUMO to the list of negative regulators of IFN signaling known to date and posits SUMO as a new regulator of IFN response.

Acknowledgments

We thank Jeanne Wietzerbin for comments and Sophie Mouillet-Richard for critical reading of the manuscript. We also thank the FACS and cell sorting platform (S2C) of the Saints-Pères Center, Paris Descartes University, for FACS analyses.

Disclosures

The authors have no financial conflicts of interest.

References

1. Borden, E. C., G. C. Sen, G. Uze, R. H. Silverman, R. M. Ransohoff, G. R. Foster, and G. R. Stark. 2007. Interferons at age 50: past, current and future impact on biomedicine. *Nat. Rev. Drug Discov.* 6: 975–990.
2. Schneider, W. M., M. D. Chevillotte, and C. M. Rice. 2014. Interferon-stimulated genes: a complex web of host defenses. *Annu. Rev. Immunol.* 32: 513–545.
3. Schindler, C., D. E. Levy, and T. Decker. 2007. JAK-STAT signaling: from interferons to cytokines. *J. Biol. Chem.* 282: 20059–20063.
4. Oudshoorn, D., G. A. Versteeg, and M. Kikkert. 2012. Regulation of the innate immune system by ubiquitin and ubiquitin-like modifiers. *Cytokine Growth Factor Rev.* 23: 273–282.
5. Gareau, J. R., and C. D. Lima. 2010. The SUMO pathway: emerging mechanisms that shape specificity, conjugation and recognition. *Nat. Rev. Mol. Cell Biol.* 11: 861–871.
6. Geiss-Friedlander, R., and F. Melchior. 2007. Concepts in sumoylation: a decade on. *Nat. Rev. Mol. Cell Biol.* 8: 947–956.
7. Rogers, R. S., C. M. Horvath, and M. J. Matunis. 2003. SUMO modification of STAT1 and its role in PIAS-mediated inhibition of gene activation. *J. Biol. Chem.* 278: 30091–30097.
8. Ungureanu, D., S. Vanhatupa, J. Grönholm, J. J. Palvimo, and O. Silvennoinen. 2005. SUMO-1 conjugation selectively modulates STAT1-mediated gene responses. *Blood* 106: 224–226.
9. Ungureanu, D., S. Vanhatupa, N. Kotaja, J. Yang, S. Aittomaki, O. A. Jänne, J. J. Palvimo, and O. Silvennoinen. 2003. PIAS proteins promote SUMO-1 conjugation to STAT1. *Blood* 102: 3311–3313.
10. Grönholm, J., S. Vanhatupa, D. Ungureanu, J. Väliaho, T. Laitinen, J. Valjakka, and O. Silvennoinen. 2012. Structure-function analysis indicates that sumoylation modulates DNA-binding activity of STAT1. *BMC Biochem.* 13: 20.
11. Begitt, A., M. Droescher, K. P. Knobeloch, and U. Vinkemeier. 2011. SUMO conjugation of STAT1 protects cells from hyperresponsiveness to IFNγ. *Blood* 118: 1002–1007.
12. Maroui, M. A., M. Pampin, and M. K. Chelbi-Alix. 2011. Promyelocytic leukemia isoform IV confers resistance to encephalomyocarditis virus via the sequestration of 3D polymerase in nuclear bodies. *J. Virol.* 85: 13164–13173.
13. Fukuda, I., A. Ito, G. Hirai, S. Nishimura, H. Kawasaki, H. Saitoh, K. Kimura, M. Sodeoka, and M. Yoshida. 2009. Ginkgolic acid inhibits protein SUMOylation by blocking formation of the E1-SUMO intermediate. *Chem. Biol.* 16: 133–140.
14. Saitoh, H., and J. Hinchey. 2000. Functional heterogeneity of small ubiquitin-related protein modifiers SUMO-1 versus SUMO-2/3. *J. Biol. Chem.* 275: 6252–6258.
15. Kessler, D. S., S. A. Veals, X. Y. Fu, and D. E. Levy. 1990. Interferon-alpha regulates nuclear translocation and DNA-binding affinity of ISGF3, a multimeric transcriptional activator. *Genes Dev.* 4: 1753–1765.
16. Chelbi-Alix, M. K., L. Pelicano, F. Quignon, M. H. Koken, L. Venturini, M. Stadler, J. Pavlovic, L. Degos, and H. de Thé. 1995. Induction of the PML protein by interferons in normal and APL cells. *Leukemia* 9: 2027–2033.
17. Stadler, M., M. K. Chelbi-Alix, M. H. Koken, L. Venturini, C. Lee, A. Saïb, F. Quignon, L. Pelicano, M. C. Guillemin, C. Schindler, et al. 1995. Transcriptional induction of the PML growth suppressor gene by interferons is mediated through an ISRE and a GAS element. *Oncogene* 11: 2565–2573.
18. Grötzinger, T., K. Jensen, and H. Will. 1996. The interferon (IFN)-stimulated gene Sp100 promoter contains an IFN-gamma activation site and an imperfect IFN-stimulated response element which mediate type I IFN inducibility. *J. Biol. Chem.* 271: 25253–25260.
19. Tatham, M. H., M. C. Geoffroy, L. Shen, A. Plechanovova, N. Hattersley, E. G. Jaffray, J. J. Palvimo, and R. T. Hay. 2008. RNF4 is a poly-SUMO-specific E3 ubiquitin ligase required for arsenic-induced PML degradation. *Nat. Cell Biol.* 10: 538–546.
20. Lallemand-Breitenbach, V., M. Jeanne, S. Benhenda, R. Nasr, M. Lei, L. Peres, J. Zhou, J. Zhu, B. Raught, and H. de Thé. 2008. Arsenic degrades PML or PML-RARalpha through a SUMO-triggered RNF4/ubiquitin-mediated pathway. *Nat. Cell Biol.* 10: 547–555.
21. El Bougrini, J., L. Dianoux, and M. K. Chelbi-Alix. 2011. PML positively regulates interferon gamma signaling. *Biochimie* 93: 389–398.
22. Herzer, K., T. G. Hofmann, A. Teufel, C. C. Schimanski, M. Moehler, S. Kanzler, H. Schulze-Bergkamen, and P. R. Galle. 2009. IFN-alpha-induced apoptosis in hepatocellular carcinoma involves promyelocytic leukemia protein and TRAIL independently of p53. *Cancer Res.* 69: 855–862.
23. Taub, D. D., A. R. Lloyd, K. Conlon, J. M. Wang, J. R. Ortaldo, A. Harada, K. Matsushima, D. J. Kelvin, and J. J. Oppenheim. 1993. Recombinant human interferon-inducible protein 10 is a chemoattractant for human monocytes and T lymphocytes and promotes T cell adhesion to endothelial cells. *J. Exp. Med.* 177: 1809–1814.
24. Sizemore, N., A. Agarwal, K. Das, N. Lerner, M. Sulak, S. Rani, R. Ransohoff, D. Shultz, and G. R. Stark. 2004. Inhibitor of kappaB kinase is required to activate a subset of interferon gamma-stimulated genes. *Proc. Natl. Acad. Sci. USA* 101: 7994–7998.
25. Gil, M. P., E. Bohn, A. K. O'Guin, C. V. Ramana, B. Levine, G. R. Stark, H. W. Virgin, and R. D. Schreiber. 2001. Biologic consequences of Stat1-independent IFN signaling. *Proc. Natl. Acad. Sci. USA* 98: 6680–6685.
26. van Boxel-Dezaire, A. H., M. R. Rani, and G. R. Stark. 2006. Complex modulation of cell type-specific signaling in response to type I interferons. *Immunity* 25: 361–372.
27. Steen, H. C., and A. M. Gamero. 2012. The role of signal transducer and activator of transcription-2 in the interferon response. *J Interferon Cytokine Res* 32: 103–110.
28. Martinez-Moczygemba, M., M. J. Gutch, D. L. French, and N. C. Reich. 1997. Distinct STAT structure promotes interaction of STAT2 with the p48 subunit of the interferon-alpha-stimulated transcription factor ISGF3. *J. Biol. Chem.* 272: 20070–20076.
29. Bluyssen, H. A., and D. E. Levy. 1997. Stat2 is a transcriptional activator that requires sequence-specific contacts provided by stat1 and p48 for stable interaction with DNA. *J. Biol. Chem.* 272: 4600–4605.
30. Begitt, A., M. Droescher, T. Meyer, C. D. Schmid, M. Baker, F. Antunes, K. P. Knobeloch, M. R. Owen, R. Naumann, T. Decker, and U. Vinkemeier. 2014. STAT1-cooperative DNA binding distinguishes type 1 from type 2 interferon signaling. *Nat. Immunol.* 15: 168–176.
31. Blaszczyk, K., A. Olejnik, H. Nowicka, L. Ozgyin, Y. L. Chen, S. Chmielewski, K. Kostyrko, J. Wesoly, B. L. Balint, C. K. Lee, and H. A. Bluyssen. 2015. STAT2/IRF9 directs a prolonged ISGF3-like transcriptional response and antiviral activity in the absence of STAT1. *Biochem. J.* 466: 511–524.
32. Duprez, E., A. J. Saurin, J. M. Desterro, V. Lallemand-Breitenbach, K. Howe, M. N. Boddy, E. Solomon, H. de Thé, R. T. Hay, and P. S. Freemont. 1999. SUMO-1 modification of the acute promyelocytic leukaemia protein PML: implications for nuclear localisation. *J. Cell Sci.* 112: 381–393.
33. Kamitani, T., K. Kito, H. P. Nguyen, H. Wada, T. Fukuda-Kamitani, and E. T. Yeh. 1998. Identification of three major sentrinization sites in PML. *J. Biol. Chem.* 273: 26675–26682.
34. Geoffroy, M. C., and M. K. Chelbi-Alix. 2011. Role of promyelocytic leukemia protein in host antiviral defense. *J Interferon Cytokine Res* 31: 145–158.
35. Nisole, S., M. A. Maroui, X. H. Mascle, M. Aubry, and M. K. Chelbi-Alix. 2013. Differential Roles of PML Isoforms. *Front. Oncol.* 3: 125.
36. Everett, R. D., and M. K. Chelbi-Alix. 2007. PML and PML nuclear bodies: implications in antiviral defence. *Biochimie* 89: 819–830.